iJRASET
International Journal For Research in Applied Science and Engineering Technology

INTERNATIONAL JOURNAL FOR RESEARCH

IN APPLIED SCIENCE & ENGINEERING TECHNOLOGY

Volume: 13 **Issue:** IV **Month of publication:** April 2025

DOI: https://doi.org/10.22214/ijraset.2025.69706

www.ijraset.com

Call: 08813907089 | E-mail ID: ijraset@gmail.com

International Journal for Research in Applied Science & Engineering Technology (IJRASET)
ISSN: 2321-9653; IC Value: 45.98; SJ Impact Factor: 7.538
Volume 13 Issue IV Apr 2025- Available at www.ijraset.com

Design of MIMO Antenna for 5G-NR Midbands (N77/ N78/ N79)

Bujjibabu Nannepaga[1], Gondru Sandeep[2], Boddu Nikitha[3], Nagireddy Deepthi[4], Mangineedu. Sravani Krishna[5], Surasani Bharath Kumar[6]

[1]*Dept. of ECE, SVUCE, Sri Venkateswara University, Tirupati, Andhra Pradesh, India*

[2, 3, 4, 5, 6]*Dept. of ECE, Lingayas Institute of Management and Technology, Madalavarigudem, Vijayawada, Andhra Pradesh, India*

Abstract: ***This present study offers to design and simulate a compact 2×2 MIMO T-slotted composite-shaped microstrip patch antenna for 5G New Radio (5G- NR) midband applications, specifically targeting bands N77, N78, and N79, operating from 3.3 GHz to 5 GHz. Using Ansys High-Frequency Structure Simulator (HFSS). The antenna was designed on an FR4 epoxy substrate with a dielectric constant (ε_r) of 4.4, thickness of 1.6 mm, and overall dimensions of 22.5 × 32 mm. The two-element antenna with no load lines achieves $S_{11} = -17.29$ dB at 4.16 GHz and $S_{22} = -21.17$ dB at 4.12 GHz, isolation (S_{12}/S_{21}) of −31.33 dB at 4.68 GHz, VSWRs of 1.32 and 1.19, radiation efficiency up to 91.59%, and bandwidths of 520 MHz (S_{11}) and 720 MHz (S_{22}). Diversity performance of the final design was evaluated and shows excellent values: Envelope Correlation Coefficient (ECC) < 0.1 across 3.3–5 GHz, Diversity Gain (DG) near 10 dB, Channel Capacity Loss (CCL) < 0.4 bits/s/Hz, Mean Effective Gain (MEG) < −3 dB, and Total Active Reflection Coefficient (TARC) < −10 dB between 4.78 GHz and 4.91 GHz.***

Keywords: ***MIMO T-slotted composite-shaped microstrip patch antenna, Envelope Correlation Coefficient, Diversity Gain, Channel Capacity Loss, VSWR.***

I. INTRODUCTION

The rapid evolution of wireless communication systems has driven the need for high-performance antenna technologies that support higher data rates, increased network capacity, and improved signal reliability. The transition from previous wireless generations to 5G technology has introduced stringent performance requirements, particularly in terms of spectrum efficiency, network scalability, and system reliability. The growing demand for 5G New Radio (5G-NR) has led to significant advancements in Multiple-Input Multiple-Output (MIMO)antenna technology, particularly for midband spectrum (3.3–5.0 GHz) applications. The N77, N78, and N79 bands provide an optimal balance between coverage, capacity, and high data rates, making them crucial for 5G base stations, IoT devices, and high-speed communication networks. MIMO antennas are essential for increasing channel capacity and enhancing communication reliability in high- frequency bands. However, designing MIMO antennas for these bands presents several challenges, including impedance mismatching, mutual coupling, poor isolation, and radiation efficiency degradation, which negatively impact overall system performance [1]. To enhance the efficiency of MIMO antennas in the 3.3–5.0 GHz range, researchers have explored various techniques such as slot-loading, defected ground structures (DGS), and decoupling networks to improve isolation, bandwidth, and diversity performance [2].

High isolation between antenna elements is essential to minimize mutual coupling, which affects key parameters like return loss, gain, and radiation efficiency. Various studies have proposed compact, high-performance MIMO antenna designs that integrate novel radiating structures to achieve low ECC (< 0.05), high diversity gain (~10 dB), and wide impedance bandwidth for 5G applications (Bujjibabu and Varadarajan, 2023) [3]. One critical aspect of MIMO antenna design is return loss (S11), which directly affects impedance matching and signal transmission efficiency. Studies have utilized machine learning models, such as Random Forest and XGBoost, to predict and optimize return loss, ensuring accurate impedance tuning for 5G antennas [4]. Additionally, diversity parameters such as Envelope Correlation Coefficient (ECC), Diversity Gain (DG), Channel Capacity Loss (CCL), Mean Effective Gain (MEG), and Total Active Reflection Coefficient (TARC) play a vital role in evaluating MIMO performance) [5]. Achieving low ECC and stable radiation efficiency ensures improved multipath fading resistance and enhanced communication reliability in 5G networks [6]. Recent review studies have analysed various MIMO antenna configurations, design methodologies, and performance enhancement techniques for 5G-NR applications. These studies highlight the importance of metamaterial-inspired, slot-integrated, and hybrid designs in improving bandwidth, isolation, and impedance matching [7]. By incorporating these insights, MIMO antennas can be further optimized for compact size, high gain, and stable performance across the 3.3–5.0 GHz spectrum.

In this paper a 2×2 MIMO antenna is designed and analysed for operation in the 3.3–5.0 GHz frequency range using High-Frequency Structure Simulator (HFSS). The focus is on optimizing return loss, isolation, gain, radiation efficiency, and diversity parameters while maintaining a compact size. The antenna aims to provide broadband coverage, reduced mutual coupling, and efficient radiation characteristics, making it highly suitable for high-speed 5G communication systems.

II. TWO ELEMENT ANTENNA WITH NO LOAD LINE DESIGN

The two-element antenna without a load line is developed by extending the single-element antenna design into a two-element configuration. In this design, the first patch is placed in its original orientation, while the second patch is rotated 180 degrees relative to the first patch. This rotation helps in achieving better isolation between the two elements by reducing mutual coupling, improving the overall diversity performance of the MIMO system, and enhancing polarization diversity for improved signal reception. It also minimizes electromagnetic interference and ensures radiation pattern symmetry, optimizing the antenna's efficiency for 5G NR midband applications. Each patch operates with a separate ground plane, ensuring independent radiation characteristics for both elements. This antenna is simulated without the integration of load lines in the ground plane. Given the resonance frequencies in the 3.68 GHz to 4.68 GHz range, this antenna is well-suited for next-generation wireless communication systems, ensuring high data rates, improved network capacity, and low latency.

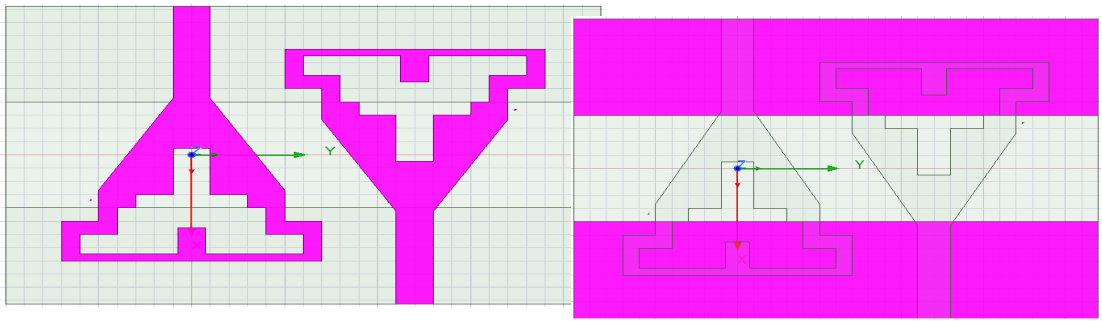

(a) (b)

Figure.1 a) Front View(b) Back view two element antenna with no load line structure

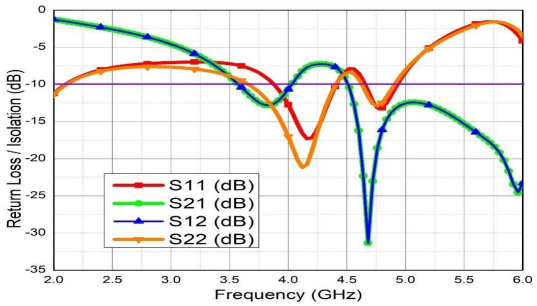

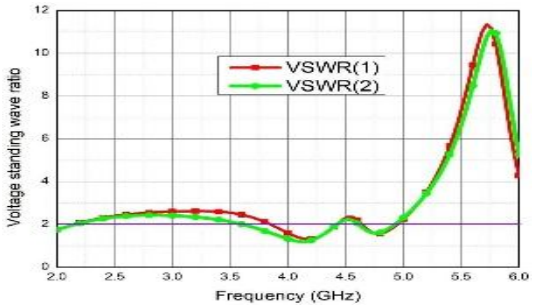

(a) (b)

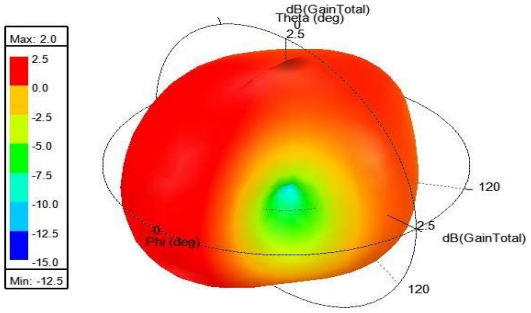

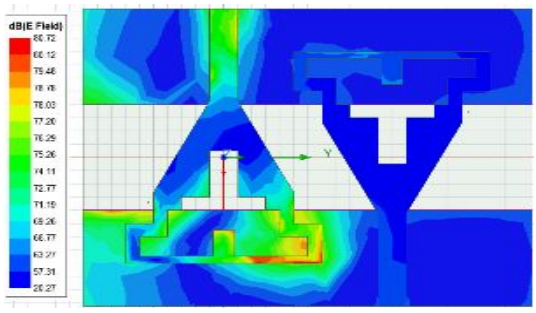

(c) (d)

Figure 2. (a) Return loss plot, (b) VSWR plot, (c) 3D Radiation plot, (d) Electric field Distribution

The antenna is designed on an FR-4 substrate with a length of 22.5 mm, width of 32 mm, height of 1.6 mm, and a dielectric constant (ε_r) of 4.4. Two ports are inserted into the antennas to facilitate the excitation and feeding of the signal to the radiating patches, ensuring efficient power transmission. Radiation box is provided to simulate a realistic open-environment condition, preventing unwanted reflections and enabling accurate analysis of the antenna's radiation characteristics. Figure 1 (a) & (b) illustrates the front and back views of the two-element antenna without a load line.

Figure 2 (a) presents the return loss (S11, S22) and isolation (S12, S21) characteristics of the two-element antenna without a load line. The Return loss (S11) parameter indicates that the first antenna resonates at 4.16 GHz, achieving a return loss of -17.29 dB, ensuring adequate impedance matching. Similarly, the S22 parameter shows that the second antenna resonates at 4.12 GHz with a return loss of -21.17 dB, reflecting efficient power transmission. The isolation parameters S12 and S21 indicate the level of coupling between the two elements, with a peak isolation of -31.33 dB at 4.68 GHz. This high isolation value confirms minimal mutual coupling, which is essential for maintaining independent operation of each antenna element. In terms of bandwidth, the S11 plot reveals an operational range from 3.88 GHz to 4.40 GHz, resulting in a bandwidth of 520 MHz. Meanwhile, the S22 plot extends from 3.68 GHz to 4.40 GHz, providing a bandwidth of 720 MHz. Given the resonance frequencies in the 3.68 GHz to 4.68 GHz range, this antenna is well-suited for next-generation wireless communication systems, ensuring high data rates, improved network capacity, and low latency.

Figure 2 (b) illustrates the Voltage Standing Wave Ratio (VSWR) representation of the two-element antenna without a load line, providing insight into its impedance matching efficiency. The red curve (VSWR(1)) represents the VSWR at Port 1, while the green curve (VSWR(2)) corresponds to Port 2. A VSWR value below 2 indicates good impedance matching, ensuring minimal signal reflection and efficient power transfer. At 4.16 GHz (VSWR(1)), the VSWR is 1.3162, confirming that Port 1 is well-matched to the 50Ω transmission line, reducing signal loss. At 4.12 GHz (VSWR(2)), the VSWR is 1.1914, demonstrating excellent impedance matching at Port 2, ensuring efficient energy transmission.

Figure 2 (c) illustrates the 3D gain radiation pattern of the two-element antenna at 4.16 GHz, depicting its directional radiation characteristics. The colour scale represents gain values, ranging from -12.5 dB (blue, lower gain regions) to 2 dB (red, higher gain regions). The red regions indicate strong radiation, while the green and blue areas correspond to lower gain levels. The radiation pattern suggests that the antenna exhibits directional radiation, efficiently radiating energy in specific directions. This characteristic makes it suitable for applications where focused gain and directional performance are essential.

Figure 2 (d) illustrates the E-field distribution of the two-element antenna without a load line, providing insight into the electric field intensity across the antenna structure. The colour scale represents the electric field strength in dB, where red and yellow regions (≈80 dB) indicate areas of high field intensity, primarily concentrated near the feedline and radiating elements. The blue regions (≈20 dB) correspond to lower field intensity, typically observed in areas with minimal electromagnetic activity. This distribution highlights the regions of strong radiation, which play a crucial role in determining the antenna's efficiency and performance in transmitting electromagnetic waves effectively.

Figure 3 (a) illustrates the Smith Chart representation of the two-element antenna without a load line, providing insight into its impedance characteristics at different frequencies. The red curve (S11) represents the reflection coefficient at Port 1, while the green curve (S12) indicates the coupling behaviour between the two ports. At 4.16 GHz, the magnitude of S11 is 0.1365, corresponding to an impedance of 1.3130 + j0.0424. This value is slightly inductive but remains close to the Smith Chart's centre, ensuring minimal signal reflection. The phase angle of 6.66° confirms that the reflected signal remains nearly in phase with the incident signal, supporting efficient power transfer. At 4.68 GHz, the magnitude of S12 is 0.0271, indicating excellent isolation between the two ports. The impedance of 0.9861 - j0.0520 is nearly purely resistive and close to an ideal 50Ω match, minimizing power loss. The corresponding signal angle of -103.50° further reinforces the high isolation performance. These impedance characteristics make this antenna well-suited for 5G mid-band (N77/N78) applications, where maintaining low reflection and strong port isolation is critical for optimal multi-element antenna performance.

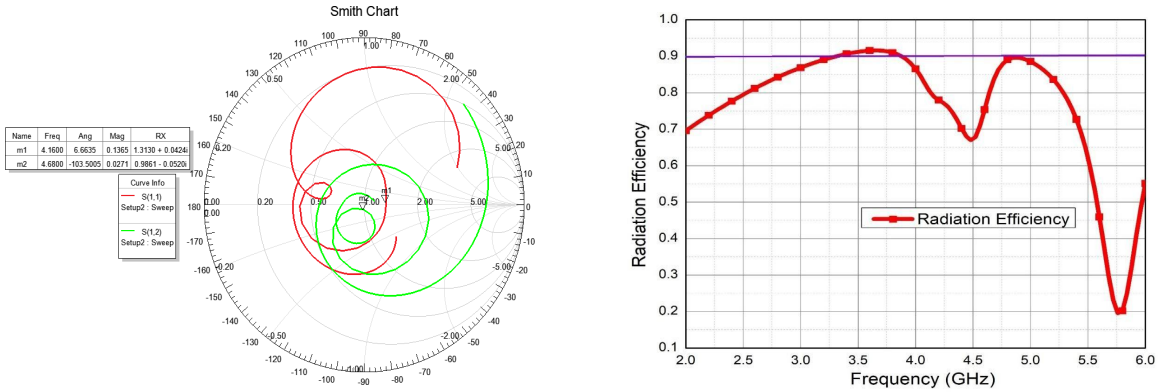

(a) (b)

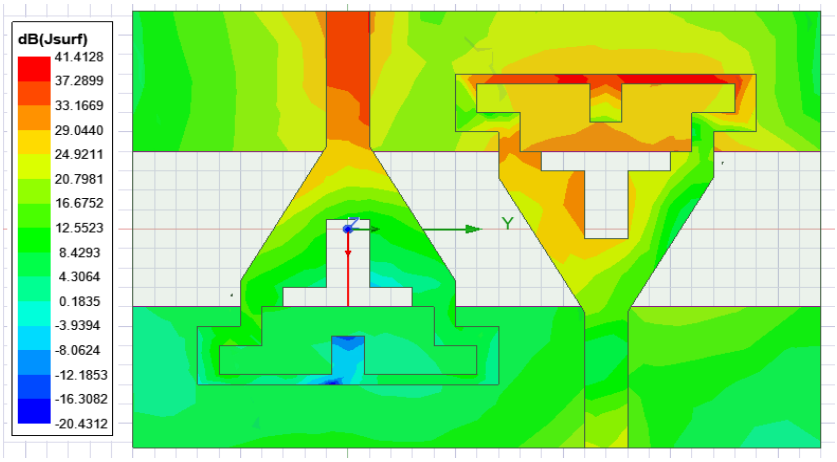

(c)

Figure 3 (a) Smith chart of two element antenna with no load line, (b) Radiation efficiency plot of two element antenna with no load line, (c) Surface current density of J-field of two element antenna with no load line.

Figure 3 (b) presents the radiation efficiency plot of the two-element antenna without a load line, illustrating its efficiency across different frequencies. For practical antenna designs, radiation efficiency above 70% is considered optimal, ensuring effective energy radiation. At 4.16 GHz, the antenna achieves 78.91% efficiency, indicating good radiation performance above the standard threshold. Similarly, at 4.12 GHz, the efficiency reaches 80.46%, further confirming strong performance. At the 3.68 GHz frequency, the radiation efficiency increases to 91.59%, demonstrating excellent efficiency with minimal losses. Likewise, at 4.88 GHz, the efficiency remains high at 89.63%, ensuring effective power radiation at this frequency.

Figure 3 (c) illustrates the J-field (surface current density) distribution of the two-element antenna without a load line, providing insight into the current flow across the antenna structure. The red regions (≈41.41 dB) indicate the highest current intensity, primarily concentrated around the feedline and specific patch edges, highlighting the critical areas contributing to signal transmission and radiation. The yellow and green regions (≈24.92 dB to 8.42 dB) represent moderate current flow, ensuring efficient operation and stable performance. In contrast, the blue regions (as low as -20.43 dB) correspond to minimal current activity, which may lead to reduced radiation in those areas. Understanding this distribution is crucial for optimizing the antenna design, minimizing unwanted losses, improving impedance matching, and enhancing overall radiation efficiency.

III.CONCLUSION

In this paper successfully presents the design, simulation of a compact 2×2 MIMO T-slotted composite-shaped microstrip patch antenna for 5G mid-band applications covering N77, N78, and N79 bands (3.3 GHz to 5 GHz). The S-parameters (S11, S22, S12, S21), VSWR, return loss, radiation efficiency, gain, smith chart, electric field (E-field) and current density (J-field) distributions were evaluated for the designed antenna. The paper demonstrates the viability of compact, efficient, and low-profile antennas

suitable for integration into 5G wireless communication systems. In the future, this antenna design can be expanded into higher-order MIMO systems such as 4×4 or 8×8 arrays to meet the increasing demand for higher data rates and enhanced spatial diversity in advanced wireless applications. These larger MIMO configurations can significantly boost signal reliability and system capacity, particularly in dense urban environments and next-generation smart communication systems. Furthermore, optimization in terms of physical structure like reducing the antenna's size without compromising performance can be achieved by adopting novel feeding mechanisms, superior substrate materials, and structural innovations. Such enhancements aim to deliver better impedance matching, higher gain, and improved isolation, ensuring the antenna remains efficient, compact, and suitable for mid-band 5G MIMO applications.

REFERENCES

[1] T. Addepalli, T. Vidyavathi, K. Neelima, M. Sharma, and D. Kumar, “Asymmetrical fed Calendula flower-shaped four-port 5G-NR band (n77, n78, and n79) MIMO antenna with high diversity performance,” Int. J. Microw. Wirel. Technol., vol. 15, no. 4, pp. 683–697, 2023, doi: 10.1017/S1759078722000800.

[2] N. S and V. Seethalakshmi, “MIMO Antenna with Isolation Enrichment for 5G Mobile Information,” Mob. Inf. Syst., vol. 2022, no. 1, p. 1802352, 2022, doi: https://doi.org/10.1155/2022/1802352.

[3] N. Bujjibabu and S. Varadarajan, “High isolated Psi-Shaped 4x4 MIMO UWB antenna for RF energy harvesting applications,” Mater. Today Proc., 2023, doi: https://doi.org/10.1016/j.matpr.2023.03.798.

[4] P. K. S. Rachit Jain, Vandana Vikas Thakery, “Employing Machine Learning Models to Predict Return Loss Precisely in 5G Antenna,” Prog. Electromagn. Res. M, vol. 118, pp. 151–161, 2023, doi: 10.2528/PIERM23062505.

[5] B. Nannepaga and S. Varadarajan, “Enhancing RF energy harvesting in smart cities with two port MIMO-UWB antenna design using machine learning algorithms,” Frequenz, vol. 78, no. 9–10, pp. 413–431, 2024, doi: doi:10.1515/freq-2023-0386.

[6] M. A. Haque et al., “Broadband high gain performance MIMO antenna array for 5 G mm-wave applications-based gain prediction using machine learning approach,” AlexandriaEng. J., vol. 104, pp. 665–679, 2024, doi: https://doi.org/10.1016 /j.aej. 2024.08.025.

[7] A. Es-saleh, M. Bendaoued, S. Lakrit, S. Das, and A. Faize, “Design aspects of MIMO antennas and its applications: A comprehensive review,” Results Eng., vol. 25, p. 103797, 2025, doi: https://doi.org/10.1016/j.rineng.2024.103797.

[8] Balanis, C. A. (2016). Antenna theory: Analysis and design (4th ed.). Wiley.

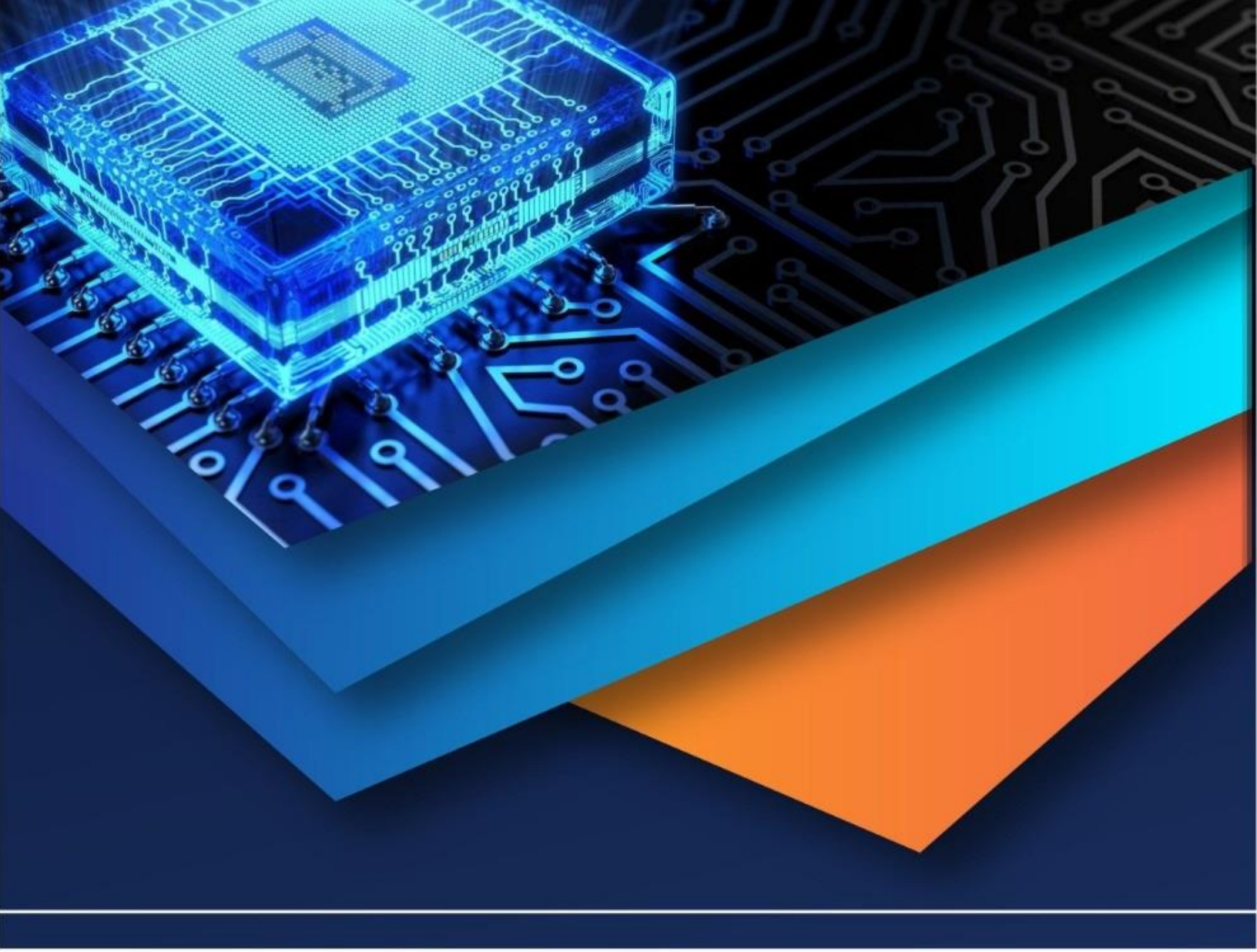

10.22214/IJRASET

45.98

IMPACT FACTOR: 7.129

IMPACT FACTOR: 7.429

INTERNATIONAL JOURNAL FOR RESEARCH

IN APPLIED SCIENCE & ENGINEERING TECHNOLOGY